RAMAN SCATTERING STUDY OF THE ALPHA-BETA PHASE TRANSITION IN QUARTZ*

Stephen M. Shapiro, Donald C. O'Shea, and Herman Z. Cummins
Department of Physics, The Johns Hopkins University, Baltimore, Maryland
(Received 19 June 1967)

The Raman spectrum of crystalline quartz has been studied at temperatures between −196 and 615°C. A weak mode of symmetry A_1 with room-temperature Raman shift of 147 cm^{-1} is found to grow in intensity and move towards zero Raman shift as the alpha-beta transition is approached. This mode, rather than the 207-cm^{-1} mode, appears to play the fundamental role in the phase transition. The temperature dependence of the Raman shift of the new mode is given by $\nu^2 \sim |T-T_c|^\gamma$ with $0.4 \leq \gamma \leq 0.5$.

Phase transitions in crystals may be viewed as arising from a breakdown of the stability criterion that all lattice modes shall have frequencies greater than 0. The microscopic theory for the case of ferroelectric phase transitions has been discussed extensively by Cochran[1,2] and by Anderson.[3] Cochran's theory leads to the prediction that the frequency of long-wavelength modes in the lowest-frequency transverse optical branch should approach 0 as T approaches the transition temperature T_c, with $\nu^2 \sim |T-T_c|$. This "soft" mode has been observed in $SrTiO_3$,[4] and recently in $KTaO_3$.[5] Ginzburg has considered the same problem from the point of view of Landau's thermodynamic theory of second-order phase transitions, and concluded that a "soft" mode should be a general characteristic of second-order phase transitions in all crystals.[6] Ginzburg specifically considered the α-β transition in quartz which was also mentioned briefly by Cochran.[2]

Quartz undergoes a transition[7] at 573°C from the low-temperature α phase with symmetry D_3 to the high-temperature β phase with symmetry D_6.[8] In the low-temperature α phase there are four totally symmetric Raman-active modes of species A_1 and eight doubly degenerate Raman-active modes of species E. The four A_1 modes have been previously assigned as 207, 356, 466, and 1081 cm^{-1}.[9] According to group theory, three of the four A_1 modes become Raman inactive (species B_1) at the transition, so that only one Raman-active mode of species A_1 is anticipated in the β phase.

The atomic motions of the lattice mode associated with the phase transition should resemble the atomic motions which transform the α structure into the β structure. Kleinman and Spitzer found that these displacements at the transition, which are of symmetry A_1, correspond closely to the 207-cm^{-1} mode.[9] Narayanaswamy observed the temperature-dependent Raman spectrum of quartz, and found that the 207-cm^{-1} line does indeed show strong variation with temperature. He found that it moves toward the Rayleigh line as the transition temperature is approached, and disappears completely in the β phase.[10] It has, therefore, been generally accepted that the 207-cm^{-1} mode is in fact the lattice vibration fundamentally associated with the α-β phase transition.

In this Letter we report new temperature-dependent Raman spectra of quartz. In our experiments an 80-mW He-Ne laser (Spectra-Physics model 125) was used as the exciting source. The scattered light was analyzed with a Spex model 1400 tandem grating monochromator and detected by an ITT FW130 photomultiplier. The photomultiplier output signal was processed with a single-channel pulse-height analyzer and linear ratemeter and recorded with a strip chart recorder.

Two approximately cubic samples (15 mm on an edge) free of optical twinning were used, both cut perpendicular to the crystal xyz axes. The sample was always oriented with the z axis normal to the scattering plane. We observed 90° scattering with incident and scattered beams normal to crystal faces so that the phonons involved were [110]. The two samples were of different origin as a check on possible sample-dependent effects, but were found to give indistinguishable spectra.

The sample was mounted in a massive double oven and heated from room temperature to over 600°C. Control could be established to within 0.1°C anywhere in the range, and the temperature was measured to within 0.05°C by a small platinum resistance thermometer placed near the sample. Because of the long time constant of the oven, temperature changes occurred very slowly and no problems were encountered with cracking of the sample at the transition. Measurements at lower tempera-

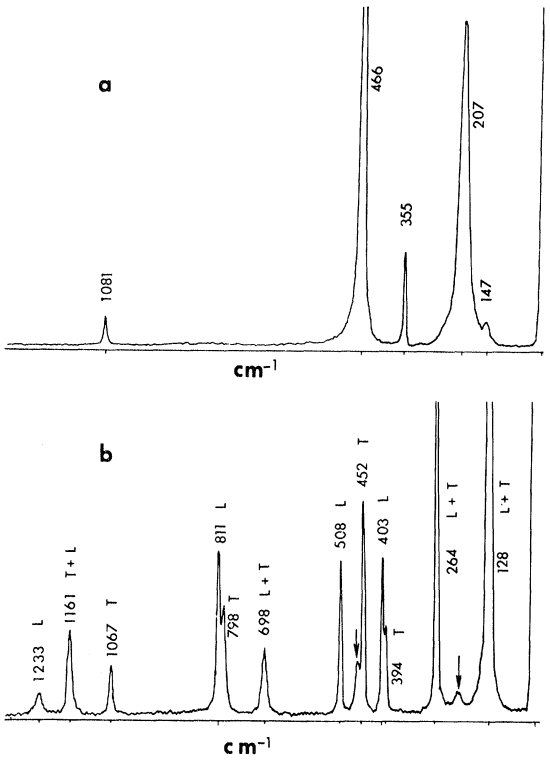

FIG. 1. Room-temperature Raman spectra of α quartz with measured values of frequencies in cm^{-1}, and Scott and Porto's (Ref. 13) polarization assignments (L = longitudinal, T = transverse). (a) The $x[zz]y$ spectrum showing the A_1 modes. (b) The $x[yx+yz]y$ spectrum showing the E modes. The arrows indicate intense A_1 modes being transmitted due to imperfect alignment.

tures were made with a conventional coldfinger Dewar.

Room-temperature quartz spectra are shown in Fig. 1. Because of the symmetry of the Raman tensors,[11] the modes of species A_1 and E can be separated easily by appropriate choice of polarization of the incident and scattered light. Figure 1(a) shows the A_1 modes (observed $x[zz]y$), while Fig. 1(b) shows the E modes (observed $x[yx+yz]y$).[12] Scott and Porto have recently studied the room-temperature spectrum of quartz in detail, and have taken explicit account of splitting of the longitudinal and transverse components of the E modes due to long-range electrostatic interactions.[13] Their polarization assignments are included above each line in Fig. 1 along with the Raman frequencies observed by us which agree, within experimental error, with those of Scott and Porto.

Figure 1(a) shows, in addition to the four

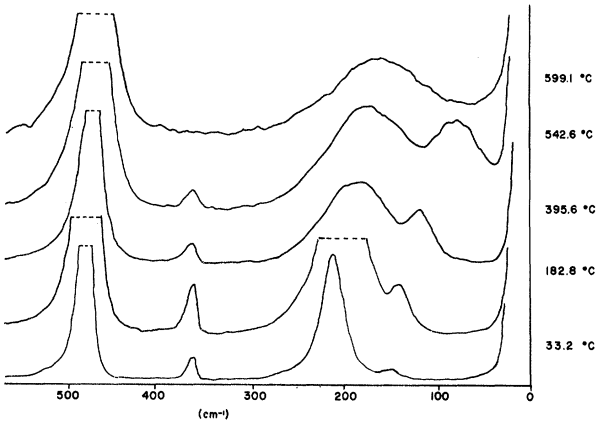

FIG. 2. 0- to 550-cm^{-1} portion of $x[zz]y$ Raman spectra at different temperatures showing four of the five totally symmetric A_1 lines of quartz. The upper spectrum is for β quartz. The gain of the lowest temperature curve is one-half that of the other curves.

A_1 lines mentioned above, an unexpected weak line at 147 cm^{-1} which was also observed by Scott and Porto.

On cooling the crystal to 78°K, the Raman shifts changed very little from the room-temperature results of Fig. 1, and the 147-cm^{-1} line was still clearly observable at 78°K. The frequencies of the E modes showed little change on heating the crystal toward the transition temperature, but the A_1 spectrum changed drastically.

Figure 2 shows the A_1 spectrum at five different temperatures (the topmost trace is in the β phase). The most striking result is the rapid increase in the intensity of the weak 147-cm^{-1} line and its corresponding decrease in frequency as the sample approaches its transition temperature. The 147-cm^{-1} line is not present in the β phase. The 207-cm^{-1} line broadens and shifts towards lower frequencies as observed by Narayanaswamy, but its frequency does not reach 0, and it is still present in the β phase as a broad band centered at 162 cm^{-1}. Of the other A_1 modes, the 466-cm^{-1} line, which is very intense at room temperature, broadens somewhat with increasing temperature but persists through the transition having shifted slightly to 459 cm^{-1} in the β phase. The 355- and 1080-cm^{-1} lines decrease continuously in intensity with increasing temperature and are not present in the β phase.

Thus, there appear to be five A_1 modes in the α phase and two in the β phase. However, group theory predicts that there should be on-

ly four A_1 modes in the α phase, and that at the phase transition three of the four A_1 modes will become Raman-inactive B_1 modes, while only one of the four will persist in the β phase as a Raman-active A_1 mode. Either the present assignments of the A_1 modes or the accepted structure must be in error. The assertion that the 147-cm^{-1} line arises from a second-order effect would contradict its apparently fundamental role in the phase transition and cannot in any case resolve the difficulty in the β phase resulting from the persistence of both the 466- and 207-cm^{-1} lines (room-temperature values).

In Fig. 3 we show the dependence of ν^2 on $T-T_c$ for the 147- and 207-cm^{-1} lines. From the logarithmic plot of the data we find for the 147-cm^{-1} mode $\nu^2 \sim |T-T_c|^{\gamma}$ with $0.4 \leq \gamma \leq 0.5$ which is to be contrasted to $\gamma = 1$ for ferroelectrics.

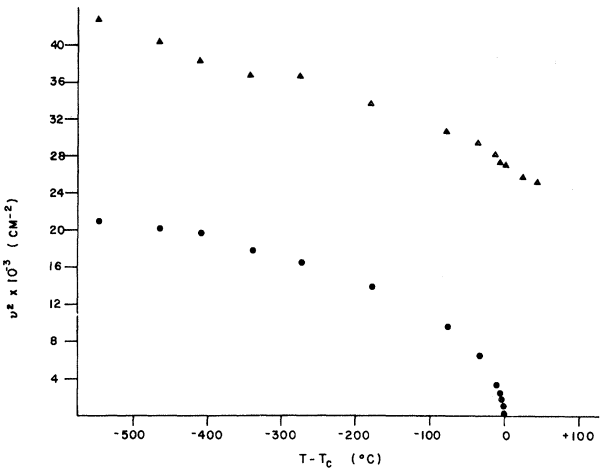

FIG. 3. ν^2 vs $T-T_c$. Solid triangles, 207-cm^{-1} (room-temperature frequency) mode; solid circles, 147-cm^{-1} (room-temperature frequency) mode.

Although no consistent explanation of the above observations is presently available, we can propose an ad hoc phenomenological model which explains the basic results:

In the β phase the silicon ions are located at hexagonal sites with the oxygens halfway between neighboring silicons. In the α phase the silicons are displaced in one of two directions along a twofold symmetry axis and the oxygens also move to one side of their β-phase sites. All the ions move in double minimum potentials centered about their β-phase sites. The double wells are strongly asymmetric due to the cooperative interaction in the (ordered) α phase so that all the ions tend to be on the same side of their double well. The two possible arrangements, depending on which side of the well has the lower energy, constitute the electrical or Dauphiné twins of quartz.[14]

Although it is usually assumed that in an untwinned crystal all unit cells have the same configuration, any one cell has a finite probability of being in the unfavorable (higher potential minimum) configuration which is proportional to the appropriate Boltzmann factor. Thus, assuming the quadratic terms of the local potential to be different at the two sites, the strong normal oscillation at 207 cm^{-1} would be accompanied by a weaker satellite at a different frequency. As the temperature is increased, the energy difference between the two configurations decreases and the intensity of the satellite line would increase, approaching that of the parent line. If, in addition, the height of the barrier decreases faster than the energy difference between the two minima, it would be the satellite whose frequency would decrease steadily towards 0 as the transition is approached.

In order to explain the persistence of the "forbidden" A_1 mode in the β phase, one might ascribe a dissymmetry to the local-potential minimum. Extensive x-ray measurements show that a double-minimum configuration with random occupation (appropriate to an order-disorder transition) in the β phase is highly unlikely.[15] Nonetheless, a small residual dissymmetry cannot be ruled out and could account for the extra A_1 mode observed in the β phase.

---

*Work supported by project DEFENDER under the joint sponsorship of Advanced Research Projects Agency, Office of Naval Research, and the Department of Defense.

[1]W. Cochran, Phys. Rev. Letters 3, 412 (1959); Advan. Phys. 9, 387 (1960).

[2]W. Cochran, Advan. Phys. 10, 401 (1961).

[3]P. W. Anderson, in Proceedings of the All-Union Conference on the Physics of Dielectrics (Academy of Sciences, USSR, Moscow, 1958), p. 290.

[4]R. A. Cowley, Phys. Rev. Letters 9, 159 (1962); A. S. Barker and M. Tinkham, Phys. Rev. 125, 1527 (1962).

[5]P. A. Fleury and J. M. Worlock, Phys. Rev. Letters 18, 665 (1967); G. Shirane, R. Nathans, and V. J. Minkiewicz, to be published.

[6]V. L. Ginzburg, Usp. Fiz. Nauk 77, 621 (1962) [translation: Soviet Phys. Usp. 5, 649 (1963)].

[7]R. B. Sosman, The Phases of Silica (Rutgers University Press, New Brunswick, New Jersey, 1965), p. 79.

[8]R. W. G. Wyckoff, Crystal Structures (Interscience

Publishers, Inc., New York, 1965), Vol. 1, pp. 312-14; B. D. Saksena, Proc. Indian Acad. Sci. A12, 93 (1940).

[9]D. A. Kleinman and W. G. Spitzer, Phys. Rev. 125, 16 (1962).

[10]P. K. Narayanaswamy, Proc. Indian Acad. Sci. A26, 521 (1947); A28, 417 (1948).

[11]R. Loudon, Advan. Phys. 13, 423 (1964).

[12]This notation follows T. C. Damen, S. P. S. Porto, and B. Tell, Phys. Rev. 142, 570 (1966).

[13]J. F. Scott and S. P. S. Porto, to be published.

[14]W. G. Cady, Piezoelectricity (Dover Publications, New York, 1962), p. 32.

[15]R. A. Young, U. S. Air Force Office of Scientific Research Final Report No. AFOSR-2569, Defense Documentation Center Report No. Ad 276235, 1962 (unpublished).

EFFECTS OF THE DEUTERON D STATE AND J DEPENDENCE IN (d,p) AND (p,d) REACTIONS

R. C. Johnson and F. D. Santos*
Physics Department, University of Surrey, London, England
(Received 10 July 1967)

It is shown that the D component of the deuteron internal wave function gives rise to corrections to the direct reaction theory of (d,p) and (p,d) reactions which depend strongly on the angular momentum of the transferred neutrons. For an orbital angular momentum transfer of 3 the corrections are large and give an important contribution to the J dependence observed in the reactions $Fe^{56}(p,d)Fe^{55}$ and $Ni^{57}(p,d)Ni^{56}$.

In the distorted-wave Born approximation (DWBA) of (d,p) and (p,d) reactions[1] the internal wave function of the deuteron φ_d appears as a factor in the transition matrix element. In all published calculations to date φ_d has been assumed to be purely S state. We present here DWBA calculations which include contributions from the D-state component of φ_d. Despite the smallness of the D-state probability[2] P_D (~7%), we find that the D state gives rise to important corrections in many cases. On the basis of these calculations we suggest that a quantitative understanding of the spin dependence of (p,d) angular distributions (J dependence)[3] will require the inclusion of D-state effects.

The deuteron wave function φ_d appears in the DWBA matrix element in the combination $V_{np}\varphi_d$, where V_{np} is the n-p potential. The evaluation of the matrix element does not require, therefore, a detailed model for V_{np}, but only an accurate functional form for φ_d. For medium energy (d,p) and (p,d) reactions it has been shown that the form[4] (normalization and phase as in Johnson[5])

$$(\tfrac{1}{2}\pi)^{1/2}(k^2+\gamma^2)U_0(k) = N[1-(k/\beta)^2], \qquad (1a)$$

$$\hbar^2\gamma^2/M = \text{Binding energy of deuteron},$$

for $U_0(k)$, the radial part of the S component of φ_d in momentum space, gives an adequate account of the contribution of $U_0(k)$ to the DWBA matrix element.[6] We have used an analogous approximation for $U_2(k)$, the radial part of the D component of φ_d in momentum space:

$$(\tfrac{1}{2}\pi)^{1/2}(k^2+\gamma^2)U_2(k) = \rho N(k/\gamma)^2. \qquad (1b)$$

In calculations in which the D state is neglected, the parameters in Eq. (1a) are usually taken to be[6]

$$N_H/(2\gamma)^{1/2} = 1.222, \quad \beta_H = 7\gamma. \qquad (2)$$

In the calculations presented here we have used parameters extracted from the wave functions of Yamaguchi,[7] which corresponds to $P_D = 4\%$. These parameters are

$$N/(2\gamma)^{1/2} = 1.244, \quad \beta = 5.76, \quad \rho = 0.028\,11. \qquad (3)$$

The differences (~3%) between these values and the equivalent parameters extracted from the Hamada-Johnston[8] wave function ($P_D \sim 7\%$) are negligible for our purposes.

Goldfarb[9] has pointed out that because N and β in Eqs. (2) and (3) are different, the D state modifies the DWBA predictions even if the explicit contribution from $U_2(k)$ is neglected. We find, however, that the latter contribution produces a much larger effect in general. In this paper calculations corresponding to zero D state will refer to the parameters given in Eq. (3).

An Algol code has been written which incorporates the D-state contribution into a standard DWBA calculation. The accuracy of the code has been checked against calculations by others,[10,11] and against suitably chosen plane-wave